Phase-flip chimera induced by environmental nonlocal coupling

V. K. Chandrasekar,[1] R. Gopal,[2,3] D. V. Senthilkumar,[4,*] and M. Lakshmanan[2]

[1]*Centre for Nonlinear Science & Engineering, School of Electrical & Electronics Engineering, SASTRA University, Thanjavur 613 401, India*
[2]*Centre for Nonlinear Dynamics, School of Physics, Bharathidasan University, Tiruchirapalli 620 024, India*
[3]*Department of Physics, Nehru Memorial College, Puthanampatti, Tiruchirapalli 621 007, India*
[4]*School of Physics, Indian Institute of Science Education and Research, Thiruvananthapuram 695 016, India*

We report the emergence of a collective dynamical state, namely, the phase-flip chimera, from an ensemble of identical nonlinear oscillators that are coupled indirectly via the dynamical variables from a common environment, which in turn are nonlocally coupled. The phase-flip chimera is characterized by the coexistence of two adjacent out-of-phase synchronized coherent domains interspersed by an incoherent domain, in which the nearby oscillators are in out-of-phase synchronized states. Attractors of the coherent domains are either from the same or from different basins of attractions, depending on whether they are periodic or chaotic. The conventional chimera precedes the phase-flip chimera in general. Further, the phase-flip chimera emerges after the completely synchronized evolution of the ensemble, in contrast to conventional chimeras, which emerge as an intermediate state between completely incoherent and coherent states. We have also characterized the observed dynamical transitions using the strength of incoherence, probability distribution of the correlation coefficient, and framework of the master stability function.

I. INTRODUCTION

The identification of an intriguing collective dynamical state, namely, the chimera state, in an ensemble of coupled identical nonlinear oscillators with nonlocal coupling [1–4] has initiated intense research activities in the recent literature [4–9]. A chimera state represents a spatially inhomogeneous state characterized by coexisting coherent and incoherent domains in an ensemble of identical oscillators. Experimentally, a chimera has also been revealed in populations of coupled chemical oscillators [10], in electro-optical systems [11], and in metronomes [12]. Real-world examples mimicking chimera states can be found in power grids [13], in unihemispheric sleep of animals [14], in multiple time scales of sleep dynamics [15], etc. Different types of chimera states such as the amplitude-mediated chimera [16] and intensity-induced chimera [17] have also been identified [18]. Recently, it has been shown that a symmetry-breaking coupling in the Stuart-Landau oscillators leads to the manifestation of chimera death [19,20]. The collective state with inhomogeneous flipping between the steady states (oscillation death) of an ensemble was called chimera death. Very recently, noise-induced coherence-resonance chimeras in a network of excitable elements were reported [21]. Coherence-resonance chimeras are associated with alternating switching of the location of coherent and incoherent domains.

In this paper, we unravel a novel dynamical regime emerging from inhomogeneous synchronized states. In particular, we consider an ensemble of identical nonlinear oscillators coupled via a common dynamic environment with nonlocal coupling. We show that the ensemble of oscillators splits into coexisting coherent and incoherent domains for appropriate strengths of the nonlocal coupling. Nearby oscillators in coherent domains exhibit in-phase synchronized oscillations, while adjacent oscillators in incoherent domains exhibit out-of-phase

oscillations. Note that the term coherent (incoherent) domains here represents the homogeneous (inhomogeneous) nature of the dynamics of the attractors in the corresponding domain and does not refer to the nature of the attractors, that is, whether they are coherent attractors with a fixed center of rotation or incoherent attractors with more than one center of rotation.

Further, we find that some of the nearby coherent domains exhibit in-phase oscillations in one of the domains and antiphase oscillations in the other, resembling the phase-flip transition [22]. Specifically, out-of-phase synchronized nearby coherent domains are interspersed by an incoherent domain (where the phases of the adjacent oscillators flip between 0 and π) at the phase-flip transition, which we call a phase-flip chimera. It is a dynamically active emerging behavior, in contrast to chimera death [19,20], where nearby oscillators populate the same branch of the inhomogeneous steady state in the coherent domain, while nearby oscillators populate different branches of the inhomogeneous steady state in the incoherent domain. Further, we find that the conventional chimera is preceded by the phase-flip chimera in addition to the other collective dynamical regimes such as coherent and synchronized states in an ensemble of paradigmatic Rössler oscillators in both the periodic and the chaotic regimes. We have used the measures strength of incoherence and probability distribution of the correlation coefficient to characterize the phase-flip chimeras and the observed dynamical transitions. In addition, we have employed the framework of the master stability function (MSF) to demarcate the synchronized and desynchronized parameter space, which agrees very well with the simulation results. It must be pointed out that the synchronized regime is a multistability regime coexisting with conventional chimeras and phase-flip chimeras depending on the distribution of the initial conditions.

The plan of the paper is as follows. We discuss the emergence of a phase-flip chimera in an ensemble of Rössler oscillators in the periodic regime in Sec. II and in the chaotic regime in Sec. III. We provide certain quantification measures

*Corresponding author: skumar@iisertvm.ac.in

such as the strength of incoherence, the probability distribution of the correlation coefficient, and the framework of the MSF to characterize the different collective dynamical behavior in the ensemble of oscillators in Sec. IV. Discussion of the global dynamical behavior in terms of two-parameter phase diagrams is provided in Sec. V. Emergence of a phase-flip chimera with global coupling among the agents in the common environment is discussed in Sec. VI and the conclusion is provided in Sec. VII. In Appendix A, we consider the effect of the relaxation time, while the effect of coupling to other variables is discussed in Appendix B.

II. PHASE-FLIP CHIMERA IN AN ENSEMBLE OF RÖSSLER OSCILLATORS IN THE PERIODIC REGIME

To elucidate the above results, we consider an ensemble of identical Rössler oscillators with a common dynamic environmental coupling represented as

$$\dot{x}_i = -y_i - z_i, \tag{1a}$$

$$\dot{y}_i = x_i + ay_i, \tag{1b}$$

$$\dot{z}_i = b + z_i(x_i - c) + kw_i, \tag{1c}$$

$$\dot{w}_i = -\alpha w_i + \frac{z_i}{2} + \frac{\varepsilon}{2P}\sum_{j=i-P}^{j=i+P}(w_j - w_i), \tag{1d}$$

$i = 1,\ldots,N$, where a, b, c, and α are the system parameters, and N is the number of oscillators in the ensemble. The oscillators in the ensemble are coupled indirectly via nonlocally coupled dynamic agents w_i in the common environment. k is the strength with which the agent w_i from the common environment interacts with the ith oscillator in the ensemble. ε is the strength of the nonlocal coupling. $P \in [1, N/2]$ is the number of nearest neighbors on each side of any oscillator in the ring with a coupling radius $r = \frac{P}{N}$. The environment or medium plays a crucial role in facilitating the complex collective dynamics such as decoherence, dissipation, and relaxation in quantum systems [23], in coordinated rhythms in biological systems [24], and in quorum sensing [25]. The

dynamics of the individual agent given by $\dot{w}_i$ in Eq. (1d) is related to the interactions of molecules between the cells and their environment [26–28]. In the following, we demonstrate the existence of a phase-flip chimera in an ensemble of Rössler oscillators in both periodic and chaotic regimes.

Individual Rössler oscillators in the ensemble exhibit periodic oscillations for the parameters $a = 0.165$, $b = 0.4$, and $c = 8.5$. We have used random initial conditions uniformly distributed between -1 and $+1$. We have fixed $N = 100$, $k = 10$, and the coupling radius r to $r = 0.3$. ($N = 100$ is chosen only for clarity, in the sense that the jumping phases can be distinctly seen. One can indeed choose any value of N for our analysis.) Snapshots of the instantaneous phases $\phi_i = \arctan(y_i/x_i)$, $i = 1, 2, \ldots, N$, and the spatiotemporal evolution of the oscillators are depicted in Fig. 1 for different values of the strength of the nonlocal coupling ε. The oscillators evolve in asynchrony for $\varepsilon = 0.02$ [see Figs. 1(a) and 1(b)], while their time-averaged frequencies are entrained [see inset in Fig. 1(a)]. Rössler oscillators being identical in the periodic regime, the frequencies of all the oscillators are always entrained (see the insets of Fig. 1) in the entire parameter regimes we have traced. Nonlocal coupling leads to the splitting of the ensemble into coexisting coherent and incoherent domains as depicted in Figs. 1(c) and 1(d) for $\varepsilon = 0.08$, thereby confirming the existence of a chimera state. Further increase in the strength of the nonlocal coupling results in the synchronous evolution of the ensemble of Rössler oscillators. Phase and complete synchronous evolution of the oscillators are clearly evident in Figs. 1(e) and 1(f), respectively, for $\varepsilon = 0.5$. The phase-flip chimera emerges after the complete synchronized state, which is illustrated in Figs. 1(g) and 1(h) for $\varepsilon = 1.5$. Phase-flip chimeras with two adjacent out-of-phase synchronized spatially coherent domains interspersed by a spatially incoherent domain are clearly evident in the spatiotemporal plot in Fig. 1(h), while their frequencies remain entrained. However, for ease of visualization the phase-flip chimera characterized by coexisting out-of-phase synchronized coherent domains (where the nearby oscillators exhibit in-phase synchronized oscillations among them in each of the synchronized domains) along with
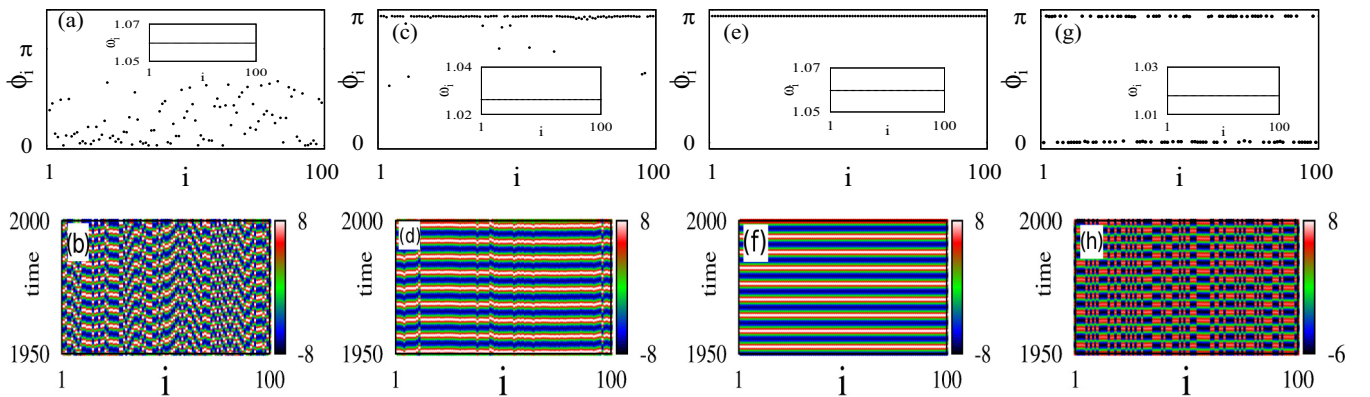

FIG. 1. Snapshots of the instantaneous phases ϕ_i (top row) and the space-time evolution (bottom row) of the ensemble of Rössler oscillators in the periodic regime for the coupling radius $r = 0.3$ of the nonlocal coupling and for different values of the strength of the nonlocal coupling, exhibiting (a, b) a desynchronized state for $\varepsilon = 0.02$, (c, d) a chimera state for $\varepsilon = 0.08$, (e, f) a synchronized state for $\varepsilon = 0.5$, and (g, h) a phase-flip chimera for $\varepsilon = 1.5$. Insets: Time-averaged frequencies of all the oscillators. Other parameter values are $a = 0.165$, $b = 0.4$, $c = 8.5$, and $\alpha = 1$.
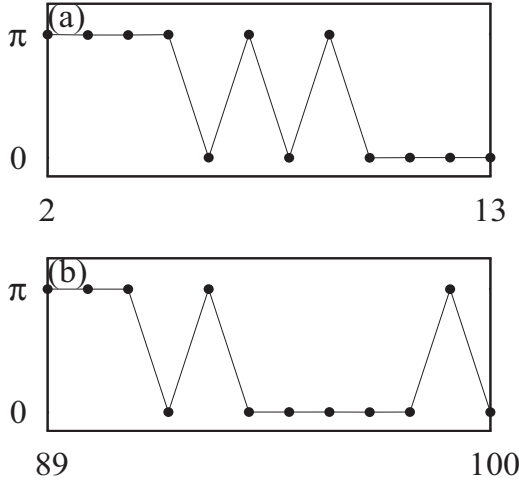
FIG. 2. Enlarged regions of Fig. 1(g) to clearly show the phase-flip chimera characterized by coexisting coherent and incoherent domains, where the nearby oscillators exhibit in-phase oscillations in the coherent domain, while the adjacent oscillators exhibit out-of-phase oscillations in the incoherent domain.

an asynchronous incoherent domain (where nearby oscillators exhibit out-of-phase synchronized oscillations) interspersing the coherent domains at the phase-flip transition is enlarged and depicted in Fig. 2 . It is noteworthy that the chimera states investigated so far have emerged as an intermediate state in the transition from completely incoherent to completely coherent states, in general. In contrast, the phase-flip chimera emerges after the completely synchronized state. Note that these are not steady states as in the case of chimera death states [19,20] but evolve dynamically, and they are also not two-cluster states, as the oscillator index cannot be reordered.

III. PHASE-FLIP CHIMERA IN AN ENSEMBLE OF RÖSSLER OSCILLATORS IN THE CHAOTIC REGIME

For the parameters $a = 0.1$, $b = 0.1$, and $c = 18.0$, the uncoupled Rössler oscillators evolve in (1) chaotically.

Snapshots of the instantaneous phases and the spatiotemporal evolution of the oscillators are depicted in Fig. 3 for different values of coupling, ε. The time-averaged frequencies of all the oscillators are shown in the insets in Fig. 3. One can observe that the frequencies of the oscillators are entrained to the same frequency as indicated by the straight line for w_i. For lower values of ε, coupled oscillators evolve in asynchrony (not shown here), whereas the ensemble of oscillators splits into coexisting coherent and incoherent domains, confirming the existence of a chimera, as shown in Figs. 3(a) and 3(b) for $\varepsilon = 0.5$. Increasing ε further, the ensemble of oscillators evolves in complete synchrony [see Figs. 3(c) and 3(d) for $\varepsilon = 1.0$]. The synchronized oscillators become desynchronized for even larger ε, the dynamics of which is illustrated in the snapshot of the instantaneous phases and the spatiotemporal plots in Figs. 3(e) and 3(f), respectively, for $\varepsilon = 1.2$. A phase-flip chimera emerges from the desynchronized state upon increasing the strength of the nonlocal coupling further as depicted in Figs. 3(g) and 3(h) for $\varepsilon = 2.5$.

The dynamics of the individual Rössler oscillators changes and plays a crucial role in the emergence of the observed collective dynamical behaviors of the ensemble of Rössler oscillators in Fig. 3 as a function of ε. The Rössler oscillators always exhibit periodic oscillations throughout the entire dynamical transition regimes of the ensemble discussed in Fig. 1, whereas in the case of chaotic oscillations of the individual oscillators the dynamical nature of the oscillators changes as discussed below. In the absence of the couplings $k = 0$ and $\varepsilon = 0$, the uncoupled individual Rössler oscillators exhibit chaotic oscillations as pointed above. A couple of uncoupled representative Rössler oscillators (namely, $N = 9$ and 13) exhibiting chaotic oscillations are depicted in Fig. 4(a). Filled circles and triangles in Fig. 4 are the Poincaré points. The value of k in the other figures [Figs. 4(b)–4(d)] is fixed at $k = 10$ as in Fig. 3. The ensemble of Rössler oscillators displays a chimera state for $\varepsilon = 0.5$ [see Fig. 3(a)]. A representative oscillator from each of the coherent and incoherent domains is displayed in Fig. 4(b). The synchronized oscillators in the coherent domain are entrained to periodic oscillations as indicated by the blue line in Fig. 4(b), while the asynchronous
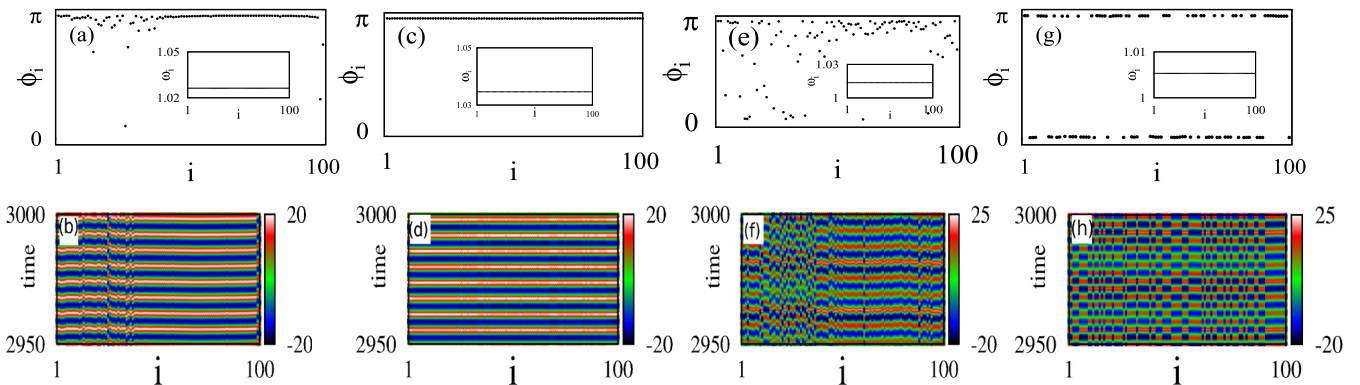

FIG. 3. Snapshots of the instantaneous phases ϕ_i (top row) and the space-time evolution (bottom row) of the ensemble of Rössler oscillators in the chaotic regime for the coupling radius $r = 0.3$ of the nonlocal coupling and for different values of the strength of the nonlocal coupling exhibiting (a, b) a chimera state for $\varepsilon = 0.5$, (c, d) a synchronized state for $\varepsilon = 1.0$, (e, f) a desynchronized state for $\varepsilon = 1.2$, and (g, h) phase-flip chimera for $\varepsilon = 2.5$. Insets: Time-averaged frequencies of all the oscillators. Other parameter values are $a = 0.1$, $b = 0.1$, $c = 18$, and $\alpha = 1$.
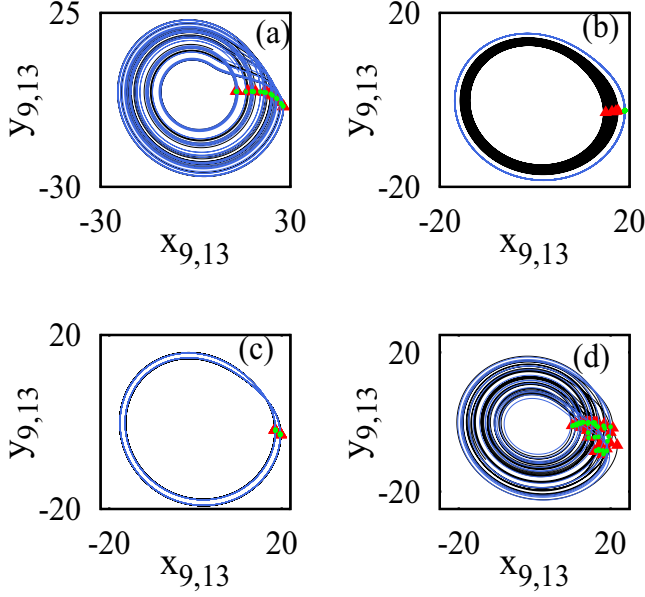
FIG. 4. Representative class of attractors along with their Poincaré points throughout the dynamical transition of the ensemble of Rössler oscillators shown in Fig. 3 as a function of the strength of the nonlocal coupling ε. (a) Desynchronized state for $\varepsilon = 0.0$, (b) chimera state for $\varepsilon = 0.5$, (c) synchronized state for $\varepsilon = 1.0$, and (d) desynchronized state for $\varepsilon = 1.2$. In (a) $k = 0$; in (c) and (d) k is fixed at 10.
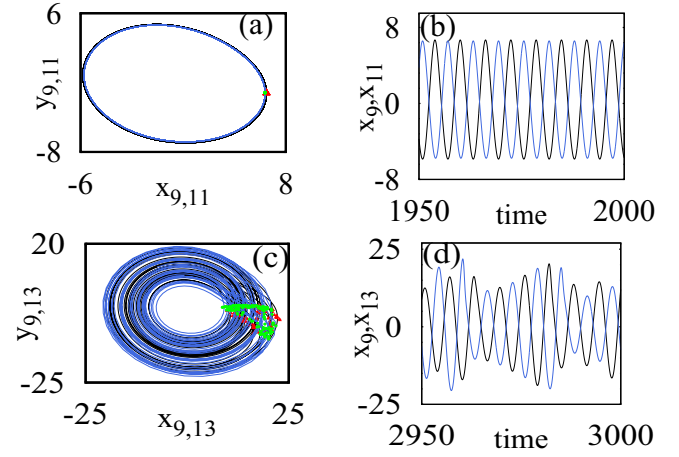

FIG. 5. Representative class of attractors along with their Poincaré points and time evolution plots of the out-of-phase synchronized coherent domains of the phase-flip chimera shown in Figs. 1(g) and 3(g). Top row: Rössler oscillators in the periodic regime. Bottom row: Rössler oscillators exhibiting chaotic oscillations.

oscillators in the incoherent domain exhibit chaotic oscillations as indicated by the black line in Fig. 4(b). The ensemble of oscillators is synchronized for the strength of the nonlocal coupling $\varepsilon = 1.0$ [see Fig. 3(c)], where the dynamics of the ensemble of oscillators become periodic as indicated by the representative oscillators in Fig. 4(c). The ensemble of Rössler oscillators is desynchronized as shown in Fig. 3(e) for $\varepsilon = 1.2$, rendering the oscillators to exhibit chaotic oscillations as displayed in Fig. 4(d), and the dynamics of the individual Rössler oscillators remain chaotic for further larger values of ε.

Attractors and the corresponding time-series plots of the representative oscillators in the out-of-phase synchronized coherent domains of the phase-flip chimera are depicted in Fig. 5. The top row represents the Rössler oscillators in the periodic regime and the bottom row corresponds to the Rössler oscillators exhibiting chaotic oscillations. Attractors exhibiting both in-phase and antiphase oscillations for the periodic case and chaotic case, along with their Poincaré points, are shown in Figs. 5(a) and 5(c), respectively. Time-series plots in Figs. 5(b) and 5(d) clearly display the out-of-phase oscillations of the two adjacent coherent domains of the phase-flip chimera.

IV. QUANTIFICATION MEASURES TO CHARACTERIZE THE CHIMERA STATES

The notion of the strength of incoherence S [17] was recently introduced by Gopal *et al.* to characterize and to

distinguish various collective dynamical states, defined as

$$S = 1 - \frac{\sum_{m=1}^{M} s_m}{M}, \quad s_m = \Theta(\delta - \sigma_l(m)), \qquad (2)$$

where $\Theta(\cdot)$ is the Heaviside step function, and δ is a predefined threshold. Normally, δ is chosen as a certain percentage value of the difference between the upper/lower bounds, $x_{l,i_{\max}}/x_{l,i_{\min}}$, of the allowed values of $x_{l,i}$. M is the number of bins of equal size $n = N/M$. The local standard deviation $\sigma_l(m)$ is introduced as

$$\sigma_l(m) = \left\langle \sqrt{\frac{1}{n} \sum_{j=n(m-1)+1}^{mn} [z_{l,j} - \langle z_{l,m} \rangle]^2} \right\rangle_t,$$
$$m = 1, 2, \ldots, M, \qquad (3)$$

where $z_{l,i} = x_{l,i} - x_{l,i+1}$, $l = 1, 2, \ldots, d$, d is the dimension of the individual unit in the ensemble, $i = 1, 2, \ldots, N$, $\langle z_{l,m} \rangle = \frac{1}{n} \sum_{j=n(m-1)+1}^{mn} z_{l,j}(t)$, and $\langle \ldots \rangle_t$ denotes the time average. When $\sigma_l(m)$ is less than δ, $s_m = 1$; otherwise, $s_m = 0$ (m in the present case is chosen as $m = 20$). The local standard deviation $\sigma_l(m)$ has some finite value in the incoherent domain $\forall m$, which is always greater than δ and hence $s_m = 0, \forall m$, thereby resulting in unit value for the strength of incoherence S in the incoherent domain. On the other hand, the standard deviation $\sigma_l(m)$ is always 0 in the coherent domain and hence $s_m = 1, \forall m$, thereby resulting in the null value of S. Since chimera states are characterized by coexisting coherent and incoherent domains, the strength of incoherence S will have values intermediate between 0 and 1, $0 < S < 1$.

The strength of incoherence is shown in Figs. 6(a) and 6(b) as a function of the strength of the nonlocal coupling ε characterizing the dynamical transition discussed in Figs. 1 and 3, respectively. The unit value of S in the range of $\varepsilon \in (0,0.08)$ in Fig. 6(a) corroborates the asynchronous evolution of the Rössler oscillators with periodic oscillations. A value of S intermediate between 0 and unity confirms the existence of a conventional chimera in the range of $\varepsilon \in (0.08,0.18)$. A null value
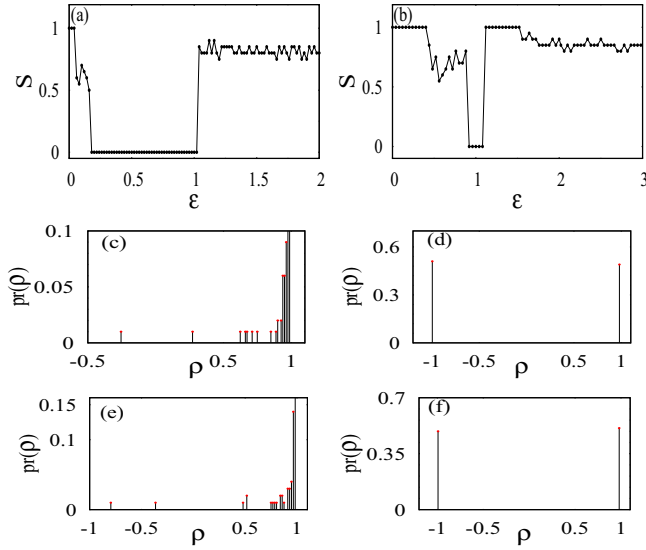
FIG. 6. Strength of the incoherence S as a function of the strength of the nonlocal coupling ε in (a) the periodic case and (b) the chaotic case. Probability distribution $\mathrm{pr}(\rho)$ of the correlation coefficient: (c) conventional chimera in the periodic case, (d) phase-flip chimera in the periodic case, (e) conventional chimera in the chaotic case, and (f) phase-flip chimera in the chaotic case.

of S in the range of $\varepsilon \in (0.18, 1.02)$ indicates synchronous evolution of the ensemble of Rössler oscillators. Fluctuations in the value of S close to unity elucidate the existence of a phase-flip chimera state. As the phase-flip chimera is characterized by out-of-phase synchronized coherent domains interspersed by an incoherent domain, most of the bins during this state have a mixture of in-phase and antiphase oscillations, while a few bins may have completely coherent (either in-phase or antiphase) oscillations leading to fluctuating values of S close to unity. Now we discuss the dynamical transition shown in Fig. 3 for chaotic oscillations of the individual Rössler oscillators in terms of the strength of incoherence S displayed in Fig. 6(b). Asynchronous evolution of the oscillators is indicated by the unit value of S in the range of $\varepsilon \in (0, 0.48)$, whereas the intermediate value of $0 < S < 1$ confirms the existence of a conventional chimera in the range of $\varepsilon \in (0.48, 0.96)$. The narrow range of the synchronized state is confirmed by $S = 0$ in the range of $\varepsilon \in (0.96, 1.04)$. The oscillators get desynchronized in the range of $\varepsilon \in (1.04, 1.66)$ as indicated by the unit value of S. Fluctuations in S close to unity beyond $\varepsilon = 1.66$ corroborate the existence of a phase-flip chimera.

We have also estimated the probability distribution of the correlation coefficient defined as

$$\rho_i = \frac{\langle (x_1(t) - \langle x_1(t) \rangle)(x_i(t + \Delta t) - \langle x_i(t) \rangle) \rangle}{\sqrt{\langle (x_1(t) - \langle x_1(t) \rangle)^2 \rangle_t \langle (x_i(t) - \langle x_i(t) \rangle)^2 \rangle_t}}, \quad (4)$$

where $i = 1, 2, \ldots, N$, to characterize the conventional chimera and phase-flip chimera. In Eq. (4), $\langle \cdot \rangle_t$ represents the time average and Δt is the time shift. The correlation coefficient is estimated by using each oscillator in the ensemble as a reference oscillator and averaging it over the number of oscillators N. The probability distribution of the correlation coefficient is depicted in Figs. 6(c)–6(f) for different values

of ε in both the periodic [Figs. 6(c) and 6(d)] and the chaotic [Figs. 6(e) and 6(f)] regimes. The correlation coefficient for completely synchronized oscillators acquires unit value and, for the antisynchronous state, reaches -1, whereas for the desynchronous state it is characterized by intermediate values between ± 1. Since the conventional chimera is characterized by the coexistence of synchronized and asynchronous domains, the probability distribution of the correlation coefficient is large near unit value and small at other values of the correlation coefficient as shown in Figs. 6(c) and 6(e). On the other hand, the phase-flip chimera is characterized by only two inhomogeneous states, namely, the in-phase and antiphase synchronized states, the correlation coefficient of the phase-flip chimera attains only $+1$ and -1 as its values. Consequently, the probability distribution of the correlation coefficient for the phase-flip chimera has only two values, $+1$ and -1, as is evident in Figs. 6(d) and 6(f).

V. TWO-PARAMETER PHASE DIAGRAMS

A two-parameter phase diagram as a function of the strength of the nonlocal coupling $\varepsilon \in (0, 2)$ and the coupling radius $r \in (0, 0.5)$ is depicted in Fig. 7(a) to gain a global
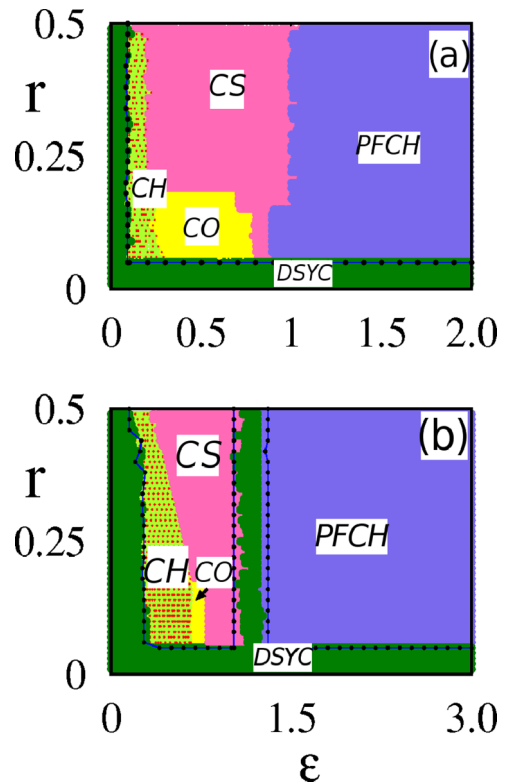

FIG. 7. Two-parameter phase diagram depicting the collective dynamical states of the ensemble of Rössler oscillators with a common dynamic environment as a function of the strength of the nonlocal coupling ε and the coupling radius r. (a) Periodic state; (b) chaotic state. Parameter spaces: DSYC, desynchronized state; CH, conventional chimera; PFCH, phase-flip chimera; CO, coherent state; and CS, complete synchronized state. Dotted lines represent the stability curves estimated from the eigenvalues of the variational equation, (8).

perspective of the collective dynamics emerging from the ensemble of Rössler oscillators exhibiting periodic oscillations in a dynamic environment with nonlocal coupling. We have used the above quantification measures discussed in Sec. IV to demarcate the different dynamical regimes of the ensemble of Rössler oscillators. The dynamical regimes delineated in Fig. 1 are indicated as DSYC, CH, SYC, and PFCH, corresponding to desynchronized states, chimera states, synchronized states, and phase-flip chimeras, respectively. In addition to the above regimes, we have found coherent states, labeled CO, where all the oscillators evolve in coherence in the range of the coupling radius $r \in (0.05, 0.2)$ and $\varepsilon \in (0.2, 0.8)$.

Using the well-known MSF formalism [33,34], the entire parameter space in Fig. 7 can be demarcated into a desynchronized state (DSYC) and a synchronous state (SYC). The stability of the synchronized manifold ($x_i = x$, $y_i = y$, $z_i = z$, and $w_i = w$; $\forall i$) is determined by the variational equations

$$\dot{\eta}_{1j} = -\eta_{2j} - \eta_{3j}, \tag{5a}$$

$$\dot{\eta}_{2j} = \eta_{1j} + a\eta_{2j}, \tag{5b}$$

$$\dot{\eta}_{3j} = \eta_{3j}(x(t) - c) + k\eta_{4j} + z(t)\eta_{1j}, \tag{5c}$$

$$\dot{\eta}_{4j} = -\alpha\eta_{4j} + \frac{\eta_{3j}}{2} + \varepsilon\lambda_j\eta_{4j}, \tag{5d}$$

where $x(t)$ and $z(t)$ are the solution of the uncoupled equation, (1). $\eta_{ik} = \zeta_i \mathbf{Q}_k$, where $\zeta_i = (\zeta_{i1}, \zeta_{i2}, \ldots, \zeta_{iN})$, and $(\zeta_1, \zeta_2, \zeta_3, \zeta_4)$ are the deviation of $(\mathbf{x}, \mathbf{y}, \mathbf{z}, \mathbf{w})$ from the synchronized solution (x, y, z, w). $\mathbf{Q}_k$ is the eigenvector of the coupling matrix G, and λ_j are the eigenvalues, where

$$G = \begin{bmatrix} a_{11} & a_{12} & a_{13} & \ldots & a_{1n} \\ a_{21} & a_{22} & a_{23} & \ldots & a_{2n} \\ \vdots & \vdots & \vdots & \ddots & \vdots \\ a_{d1} & a_{d2} & a_{d3} & \ldots & a_{dn} \end{bmatrix}, \tag{6}$$

with $a_{ii} = -1$ and $a_{i(i+j)} = a_{i(i-j)} = \frac{1}{2P}$ for $i = 1, 2, \ldots, N$ and $j = 1, 2, \ldots, P$. Here $a_{i(N+k)} = a_{ik}$ and $a_{i(1-k)} = a_{i(N-k+1)}$ for $k = 1, 2, \ldots, P$. The eigenvalues are given by

$$\lambda_j = -1 + \frac{1}{P}\sum_{k=1}^{P}\cos\left(\frac{2\pi k}{N}j\right), \quad j = 0, 1, 2, \ldots, N-1. \tag{7}$$

The eigenvalue λ_0 corresponds to the perturbation parallel to the synchronization manifold, while the other $N-1$ eigenvalues correspond to the perturbation transverse to the synchronization manifold. The transverse eigenmodes should be damped out to have a stable synchronization manifold. The stability of the synchronization manifold depends only on the largest eigenvalue $\lambda_1 = -1 + \frac{1}{P}\sum_{k=1}^{P}\cos(\frac{2\pi k}{N})$, and the corresponding variational equation becomes

$$\dot{\eta}_{11} = -\eta_{21} - \eta_{31}, \quad \dot{\eta}_{21} = \eta_{11} + a\eta_{21},$$

$$\dot{\eta}_{31} = \eta_{31}(x(t) - c) + k\eta_{41} + z(t)\eta_{11},$$

$$\dot{\eta}_{41} = -\alpha\eta_{41} + \frac{\eta_{31}}{2} - \varepsilon\left(1 - \frac{1}{P}\sum_{k=1}^{P}\cos\left(\frac{2\pi k}{N}\right)\right)\eta_{41}. \tag{8}$$
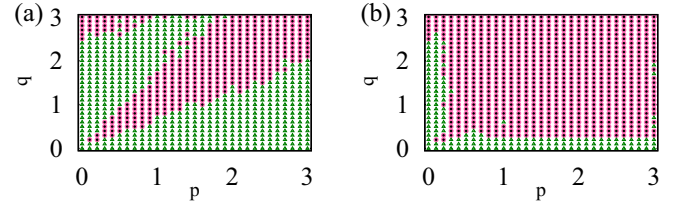

FIG. 8. Basin of attraction depicting the coexisting phase-flip chimera (red circles) and complete synchronized states (green triangles) in (a) periodic and (b) chaotic cases of the coupled Rössler oscillators.

Now, the value of the largest Lyapunov exponent of the variational equation, (8), for each value of the parameters in the two-parameter phase diagram (Fig. 7) is used to demarcate the two-parameter phase diagram into a desynchronized state (DSYC) and a synchronous state (SYC) as indicated by the dotted lines in Fig. 7(a). Before the dotted lines the largest Lyapunov exponent acquires positive values, while for the parameters above the dotted lines it acquires negative values, indicating the stability of the synchronization manifold. Figure 7 elucidates that the simulation results are in agreement with the results obtained using the semianalytic approach, namely, the MSF formalism, in demarcating the synchronized and desynchronized regimes. It should be noted that the synchronous state is a multistable state with coexisting chimera states, coherent states, and phase-flip chimeras, depending on the distribution of the initial conditions (for a given choice of ϵ and r or ϵ and k). The multistable nature of the synchronized parameter space coexisting with the phase-flip chimera is shown in Fig. 8.

A similar two-parameter phase diagram in the range of $\varepsilon \in (0, 3)$ and $r \in (0, 0.5]$ of the ensemble of Rössler oscillators exhibiting chaotic oscillations is shown in Fig. 7(b). The main difference in the emergent dynamics from the ensemble of Rössler oscillators with periodic oscillations [see Fig. 7(a)] versus that with chaotic oscillations [see Fig. 7(b)] is that in the latter case the phase-flip chimera (labeled PFCH) is immediately preceded by asynchronous oscillations (labeled DSYC) of the ensemble. That is, the dynamical transition occurs in the sequence desynchronized state (DSYC), chimera state (CH), coherent state (CO) or completely synchronized state (SYC), depending on the value of r, again DSYC, and, finally, phase-flip chimera (PFCH) as a function of ε, which is evident from the two-parameter phase diagram in Fig. 7(b). The synchronized and desynchronized parameter space is also demarcated by solving the variational equation, Eq. (8), as indicated by the dotted lines in Fig. 7. There, the parameter space within the dotted lines is characterized by negative values of the largest Lyapunov exponent of the variational equations, indicating a stable synchronized state. It is noteworthy that in both the two-parameter phase diagrams, the discussed transition occurs for $r > 0.05$, below which the ensemble of oscillators remains in the asynchronous state, elucidating that the phase-flip chimera may not emerge in the nearest-neighbor coupling between the agents. It also reveals that an appropriate coupling radius is necessary for emergence of the phase-flip chimera.

In order to demonstrate the stability of the phase-flip chimera, we have depicted the basin of attraction of the
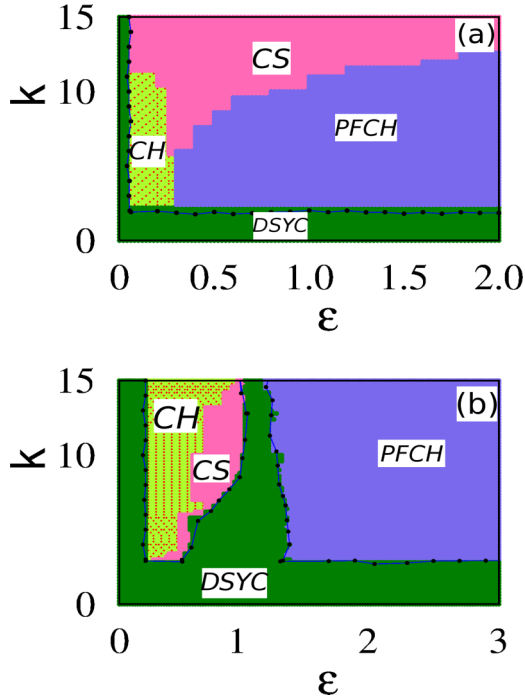
FIG. 9. Two-parameter phase diagram depicting the collective dynamical states of the ensemble of Rössler oscillators with a common dynamic environment as a function of k and ε. Parameter spaces: DSYC, desynchronized state; CH, conventional chimera; PFCH; phase-flip chimera, and CS, complete synchronized state. Dotted lines represent the stability curves estimated from the eigenvalues of the variational equation, (8).

ensemble, Eq. (1), in Fig. 8 as a function of p and q, which correspond to the initial conditions of the x and y variables. The initial conditions for the variables z and w are uniform random numbers distributed between -1 and 1, whereas those for the x and y variables are uniform random numbers distributed between $\pm p$ and $\pm q$, respectively. It is clear that both the phase-flip chimeras (indicated by circles) and the completely synchronized states (indicated by triangles) coexist for a wide choice of initial conditions, corroborating the stability and robustness of the phase-flip chimera.

To explore the effect of environmental coupling on the observed dynamical transition in detail, we have plotted the two-parameter phase diagram as a function of the strength of the nonlocal coupling ε and the strength k with which the local agents interact with their respective oscillators in Figs. 9(a) and 9(b) for periodic and chaotic oscillations of individual uncoupled Rössler oscillators, respectively. The parameter spaces leading to the desynchronous state (DSYC), conventional chimera (CH), phase-flip chimera (PFCH), and complete synchronous (CS) state are labeled in both figures. Asynchronous and completely synchronous parameter spaces are also demarcated (indicated by dotted lines) using the value of the largest Lyapunov exponent of the variational equation, (8). In the periodic regime of the Rössler oscillators, the coupled oscillators remain asynchronous in the entire range of ε for small values of k as shown in Fig. 9(a). In the range of $k \in (2.1, 5.6)$, the desynchronized state is followed by a conventional chimera and a phase-flip chimera as ε

is increased. Increasing k further, the conventional chimera and phase-flip chimera regimes are separated by a complete synchronized regime up to $k = 12.6$. A transition from an asynchronous to a complete synchronized state occurs for $k > 12.6$ as a function of ε. Thus the emergence of the phase-flip chimera is spread over a wide range of $k \in (2.1, 12.6)$ and ε. For chaotic oscillations of individual Rössler oscillators, we have observed transitions similar to those in Fig. 9(a) as a function of k and ε, except for the fact that the range of the phase-flip chimera extends to a much wider range of k and ε [see Fig. 9(b)], while the desynchronized state precedes the phase-flip chimera.

The existence of phase-flip transition in two coupled oscillators induced by the environmental coupling in Eq. (1) was shown in [27] and [28]. We find that environmental coupling among the agents and the oscillators induces a phase-flip transition and bifurcation, while nonlocal coupling among the agents in the common environment facilitates the onset of an incoherent domain at the phase-flip transition. In the absence (or for low values of the strength) of environmental coupling one cannot observe a phase-flip chimera as is evident from the two-phase diagram in Fig. 9. We have also found that the emergence of the phase-flip chimera depends on the relaxation time of the environmental coupling in Eq. 1(d) and the phase-flip chimera emerges for the parameter $\alpha \geqslant 1$, which determines the relaxation time of the external agent w_i (see Appendix A for more details).

VI. PHASE-FLIP CHIMERA WITH GLOBALLY COUPLED AGENTS

It is also noteworthy that we have identified the emergence of a phase-flip chimera in the case of globally coupled agents. Snapshots of the instantaneous phases ϕ_i and the space-time evolution of the ensemble of Rössler oscillators in the chaotic regime but with global coupling between the agents for the value of the strength of the global coupling $\varepsilon = 2.5$ are shown in Fig. 10. The value of the other parameters and the distribution of the initial conditions are the same as in Fig. 3. It is clear from the figure that the phase-flip chimera characterized by two adjacent out-of-phase synchronized coherent domains, where nearby oscillators are exhibiting in-phase synchronized oscillations, interspersed by an incoherent domain, where nearby oscillators exhibit out-of-phase oscillations (see the inset in Fig. 10), exists even with global coupling between the agents in the common environment. We have also confirmed the emergence of a phase-flip chimera from the ensemble for periodic oscillations
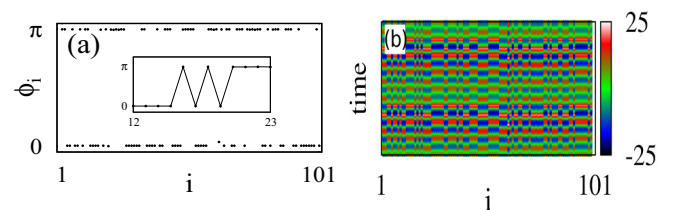

FIG. 10. (a) Snapshots of the instantaneous phases ϕ_i and (b) the space-time evolution of the ensemble of Rössler oscillators in the chaotic regime with global coupling between the agents for the value of the strength of the global coupling $\varepsilon = 2.5$.

of individual Rössler oscillators with global coupling between the agents. It is known that in an ensemble of globally coupled oscillators one can reorder the spatial index of the oscillators such that the spatial inhomogeneity with coexisting in-phase and out-of-phase synchronized oscillators in the phase-flip chimera state (see Fig. 2) can be recast as a two-cluster state [35–37]. However, we would like to point out that once the spatial ordering of the globally coupled oscillators is fixed by indexing them from 1 to N, then the distribution of initial conditions as stated above among the oscillators results in spatially inhomogeneous states with coherent out-of-phase synchronized domains interspersed by an incoherent domain comprised of nearby oscillators exhibiting in-phase and antiphase oscillations. This confirms the emergence of a phase-flip chimera even with global coupling among the agents. Indeed, several recent investigations have reported the existence of chimera states in an ensemble of globally coupled oscillators [17,18,29–32].

Finally, we have also checked whether phase-flip chimeras occur when the coupling is additionally given to the x or y variables, that is, to Eq. (1a) or Eq. (1b). In these cases only the transition from a desynchronized state to a synchronized state occurs (see Appendix B for more details).

VII. CONCLUSIONS

To summarize, we have identified an interesting type of collective dynamical regime, called phase-flip chimeras, in an ensemble of identical Rössler oscillators coupled indirectly via the agents from a common dynamic environment, where the agents are coupled nonlocally with coupling radius r. Such interactions are found in the diffusion of biomolecules between cells and their environment [26]. The phase-flip chimera is characterized by two out-of-phase synchronized spatially coherent domains interspersed with a spatially incoherent domain comprised of nearby oscillators exhibiting out-of-phase oscillations. The oscillators in each of the coherent domains exhibit phase-synchronized oscillations among themselves, whereas the two adjacent coherent domains in the phase-flip chimera exhibit out-of-phase synchronized oscillations. The robustness of the phase-flip chimera is also confirmed by depicting its occurrence over a wide range of parameters using the two-parameter phase diagram. Further, it is also shown that the phase-flip chimera is preceded by the conventional chimera and it emerges only after the completely synchronized state emerges. In the chaotic regime the phase-flip chimera is immediately preceded by an asynchronous state, which in turn emerges as a desynchronized state from the synchronous evolution of the ensemble of oscillators. We have used the strength of incoherence, probability distribution of the correlation coeffecient, and MSF to characterize the observed dynamical transition of the ensemble of Rössler oscillators. It is also confirmed that the phase-flip chimera emerges even with global coupling among the agents, whereas with nearest-neighbor coupling such a state does not emerge.

APPENDIX A: RELAXATION TIME OF THE ENVIRONMENTAL COUPLING, EQ. (1d)

The dependence of the dynamics of the oscillators on the relaxation time is depicted in Fig. 11. The dynamics of the agent w_1 (as an example) is shown in Fig. 11(a) for $\varepsilon = 0$ and in Fig. 11(b) for $\varepsilon = 1.5$. The dynamics of randomly chosen
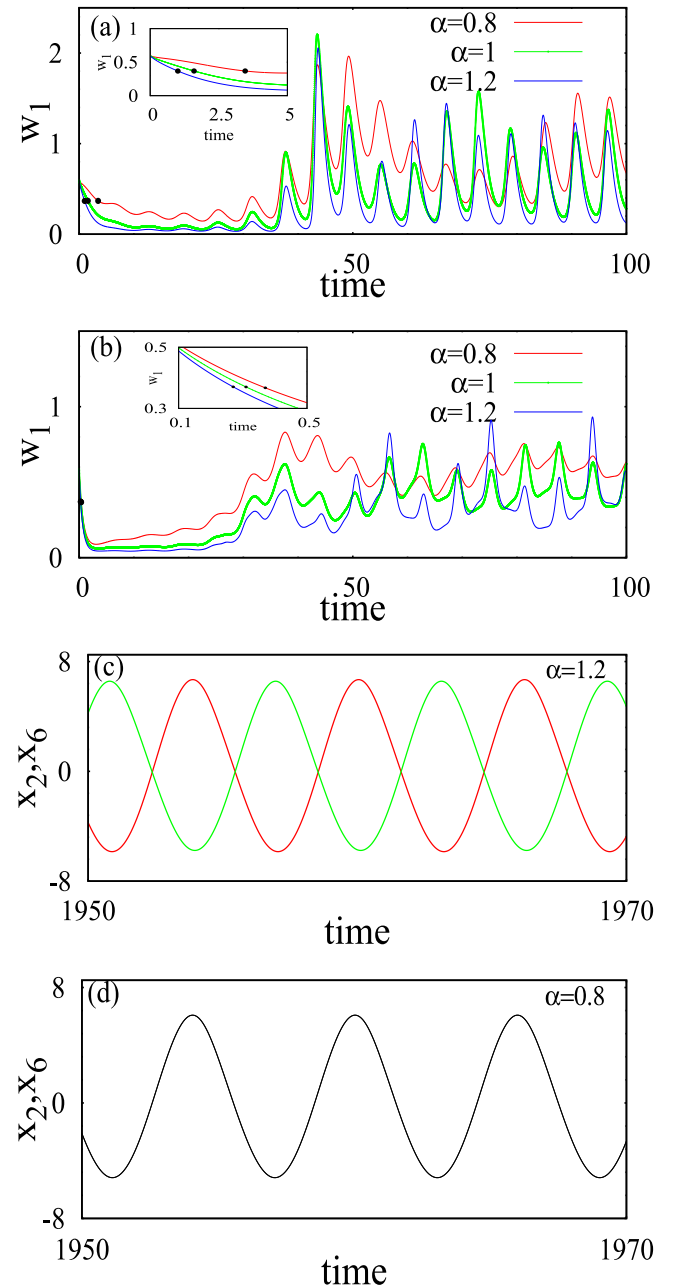

FIG. 11. Dynamics of the agent w_1 (a) for $\varepsilon = 0$ and (b) for $\varepsilon = 1.5$, with $k = 10$. (c, d) Dynamics of random oscillators for different values of the relaxation parameter α.

oscillators is shown in Figs. 11(c) and 11(d) for different values of the relaxation parameter α occurring in Eq. (1d).

As the value of the parameter α is increased the relaxation time (pointed out by filled circles in the insets) decreases both in the absence (Fig. 11(a)) and in the presence (Fig. 11(b)) of coupling between agents w_i in Eq. (1d). It should be noted that the relaxation time is very much lower in the presence of coupling between the oscillators [see Fig. 11(b)] compared to uncoupled oscillators [see Fig. 11(a)]. Further, the value of the parameter α, which determines the relaxation time, dictates the collective behavior of the ensemble of oscillators. Phase-flip chimeras are observed for $\alpha \geqslant 1$. For $\alpha = 1$ the phase-flip chimera is shown in Figs. 1 and 3. For $\alpha > 1.2$, the out-of-phase oscillations of the adjacent out-of-phase synchronized coherent domains of the phase-flip chimera are represented by a couple of representative oscillators in Fig. 11(c). On the other hand, for $\alpha < 1.0$, we observe only a synchronized state for any choice of initial conditions and coupling strength as shown by the representative oscillators in Fig. 11(d). Thus we find that the emergence of the phase-flip chimera depends on the relaxation time of the environmental coupling in Eq. (1d) and that it emerges for parameter $\alpha \geqslant 1$, which determines the relaxation time of the w_i's.

APPENDIX B: DYNAMICS OF COUPLING WITH OTHER VARIABLES

We have also examined the typical transition from a desynchronized state to a synchronized states by coupling the agent w_i to other variables, x_i or y_i, in the same fashion as in Eq. (1d). Snapshots of the instantaneous phases ϕ_i of the ensemble of Rössler oscillators coupled via the y variable are shown in Fig. 12. The left column corresponds to the case of periodic oscillations when the oscillators are uncoupled, while the right column corresponds to the case of chaotic oscillations of uncoupled oscillators. A desynchronized state is observed for $\varepsilon = 0.005$ [see Fig. 12(a)] for the case of periodic
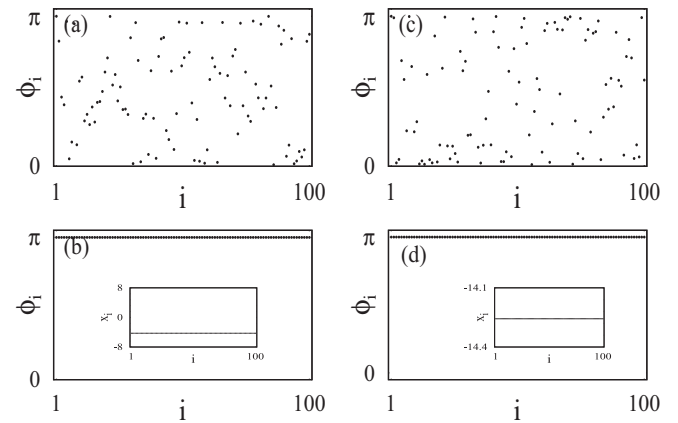

FIG. 12. Snapshots of the instantaneous phases ϕ_i of the ensemble of Rössler oscillators coupled via the y variable displaying (a) a desynchronized state for $\varepsilon = 0.005$, (b) a completely synchronized state for $\varepsilon = 0.02$, (c) a desynchronized state for $\varepsilon = 0.005$, and (d) a completely synchronized state for $\varepsilon = 0.04$. Left column: Periodic oscillations of Rössler oscillators. Right column: Chaotic oscillations of Rössler oscillators. Insets in (b) and (d): Snapshots of x_i.

oscillations. With an increase in the coupling strength the oscillators are completely synchronized as shown in Fig. 12(b) for $\varepsilon = 0.02$ and remain synchronized for any high coupling strength. For the case of chaotic oscillations of uncoupled Rössler oscillators, the oscillators are desynchronized for low values of the coupling strength as shown in Fig. 12(c) for $\varepsilon = 0.005$ and remain completely synchronized above a threshold value of ε as illustrated in Fig. 12(d) for $\varepsilon = 0.04$. Hence, only the existence of a completely synchronized state from the desynchronized state is found and we are not able to find a phase-flip chimera for any value of k and ε. A similar scenario arises for x coupling as well (which we do not present here).

[1] Y. Kuramoto, *Chemical Oscillations, Waves, and Turbulence* (Springer-Verlag, Berlin, 1984).

[2] A. Pikovsky, M. Rosenblum, and J. Kurths, *Synchronization: A Universal Concept in Nonlinear Sciences* (Cambridge University Press, Cambridge, UK, 2001).

[3] A. T. Winfree, *The Geometry of Biological Time* (Springer, New York, 2001).

[4] D. Battogtokh and Y. Kuramoto, Nonlinear Phenom. Complex Syst. **5**, 380 (2002); D. M. Abrams and S. H. Strogatz, Phys. Rev. Lett. **93**, 174102 (2004); D. M. Abrams, R. Mirollo, S. H. Strogatz, and D. A. Wiley, *ibid.* **101**, 084103 (2008); G. C. Sethia, A. Sen, and F. M. Atay, *ibid.* **100**, 144102 (2008); M. J. Panaggio and D. M. Abrams, Nonlinearity **28**, R67 (2015).

[5] C. R. Laing and C. C. Chow, Neural Comput. **13**, 1473 (2000); C. R. Laing, Phys. Rev. E **81**, 066221 (2010); G. Bordyugov, A. Pikovsky, and M. Rosenblum, *ibid.* **82**, 035205 (2010); S. Olmi, A. Politi, and A. Torcini, Europhys. Lett. **92**, 60007 (2010).

[6] I. Omelchenko, Y. Maistrenko, P. Hövel, and E. Schöll, Phys. Rev. Lett. **106**, 234102 (2011); I. Omelchenko, B. Riemen-

schneider, P. Hövel, Y. Maistrenko, and E. Schöll, Phys. Rev. E **85**, 026212 (2012); I. Omelchenko, O. E. Omelchenko, P. Hövel, and E. Schöll, Phys. Rev. Lett. **110**, 224101 (2013).

[7] J. H. Sheeba, V. K. Chandrasekar, and M. Lakshmanan, Phys. Rev. E **79**, 055203(R) (2009); **81**, 046203 (2010).

[8] S. R. Ujjwal and R. Ramaswamy, Phys. Rev. E **88**, 032902 (2013); D. Pazo and E. Montbrió, Phys. Rev. X **4**, 011009 (2014); L. Schmidt, K. Schönleber, K. Krischer, and V. García Morales, Chaos **24**, 013102 (2014).

[9] V. K. Chandrasekar, R. Suresh, D. V. Senthilkumar, and M. Lakshmanan, Europhys. Lett. **111**, 60008 (2015); B. K. Bera, D. Ghosh, and M. Lakshmanan, Phys. Rev. E **93**, 012205 (2016).

[10] M. R. Tinsley, S. Nkomo, and S. Showalter, Nat. Phys. **8**, 662 (2012); S. Nkomo, M. R. Tinsley, and K. Showalter, Phys. Rev. Lett. **110**, 244102 (2013).

[11] A. M. Hagerstrom, T. E. Murphy, R. Roy, P. Hövel, I. Omelchenko, and E. Schöll, Nat. Phys. **8**, 658 (2012).

[12] E. A. Martens, S. Thutupalli, A. Fourriére, and O. Hallatschek, Proc. Natl. Acad. Sci. USA **110**, 10563 (2013).

[13] G. Filatrella, A. H. Nielsen, and N. F. Pedersen, Eur. Phys. J. B **61**, 485 (2008).

[14] N. C. Rottenberg, C. J. Amlaner, and S. L. Lima, Neurosci. Biobehav. Rev. **24**, 817 (2000).

[15] E. Olbrich, J. C. Claussen, and P. Achermann, Philos. Trans. R. Soc. London A **369**, 3884 (2011)

[16] G. C. Sethia, A. Sen, and G. L. Johnston, Phys. Rev. E **88**, 042917 (2013).

[17] V. K. Chandrasekar, R. Gopal, A. Venkatesan, and M. Lakshmanan, Phys. Rev. E **90**, 062913 (2014).

[18] G. C. Sethia and A. Sen, Phys. Rev. Lett. **112**, 144101 (2014); A. Yeldesbay, A. Pikovsky, and M. Rosenblum, ibid. **112**, 144103 (2014).

[19] A. Zakharova, M. Kapeller, and E. Schöll, Phys. Rev. Lett. **112**, 154101 (2014); J. Phys. Conf. Ser. (to be published).

[20] K. Premalatha, V. K. Chandrasekar, M. Senthilvelan, and M. Lakshmanan, Phys. Rev. E **91**, 052915 (2015); **93**, 052213 (2016).

[21] N. Semenova, A. Zakharova, V. Anishchenko, and E. Schöll, arXiv:1512.07036v1.

[22] J. M. Cruz, J. Escalona, P. Parmananda, R. Karnatak, A. Prasad, and R. Ramaswamy, Phys. Rev. E **81**, 046213 (2010); A. Prasad, J. Kurths, S. K. Dana, and R. Ramaswamy, ibid. **74**, 035204 (2006); A. Sharma, M. D. Shrimali, A. Prasad, R. Ramaswamy, and U. Feudel, ibid. **84**, 016226 (2011).

[23] H. Ammann, R. Gray, I. Shvarchuck, and N. Christensen, Phys. Rev. Lett. **80**, 4111 (1998); W. H. Zurek, S. Habib, and J. P. Paz, ibid. **70**, 1187 (1993); S. A. Gurvitz, L. Fedichkin, D. Mozyrsky, and G. P. Berman, ibid. **91**, 066801 (2003); S. Braig and K. Flensberg, Phys. Rev. B **68**, 205324 (2003).

[24] A. Kuznetsov, M. Kærn, and N. Kopell, SIAM J. Appl. Math. **65**, 392 (2004); R. Wang and L. Chen, J. Biol. Rhythms **20**, 257 (2005); D. Gonze, S. Bernard, C. Waltermann, A. Kramer, and H. Herzel, Biophys. J. **89**, 120 (2005).

[25] B. W. Li, C. Fu, H. Zhang, and X. Wang, Phys. Rev. E **86**, 046207 (2012).

[26] E. Ullner, A. Zaikin, E. I. Volkov, and J. Garcia-Ojalvo, Phys. Rev. Lett. **99**, 148103 (2007); E. Ullner, A. Koseska, J. Kurths, E. Volkov, H. Kantz, and J. Garcia-Ojalvo, Phys. Rev. E **78**, 031904 (2008).

[27] V. Resmi, G. Ambika, and R. E. Amritkar, Phys. Rev. E **81**, 046216 (2010).

[28] A. Sharma, M. D. Shrimali, and S. K. Dana, Chaos **22**, 023147 (2012).

[29] T. Banerjee and D. Ghosh, Phys. Rev. E **89**, 052912 (2014).

[30] L. Schmidt and K. Krischer, Phys. Rev. Lett. **114**, 034101 (2015).

[31] L. Schmidt and K. Krischer, Chaos **25**, 064401 (2015).

[32] M. I. Bolotov, G. V. Osipov, and A. Pikovsky, Phys. Rev. E **93**, 032202 (2016).

[33] L. M. Pecora and T. L. Carroll, Phys. Rev. Lett. **80**, 2109 (1998).

[34] S. Acharyya and R. E. Amritkar, Phys. Rev. E **92**, 052902 (2015).

[35] S. C. Manrubia, A. S. Mikfailov, and O. D. Zanatte, Emergence of Dynamical Order: Synchronization Phenomena in Complex Systems (World Scientific, Singapore, 2004).

[36] K. Okuda, Physica D **63**, 424 (1993); V. Hakim and W.-J. Rappel, Phys. Rev. A **46**, R7347 (1992); N. Nakagawa and Y. Kuramoto, Prog. Theor. Phys. **89**, 313 (1993); Y. Kuramoto, ibid. **94**, 321 (1995).

[37] D. H. Zanette and A. S. Mikhailov, Phys. Rev. E **57**, 276 (1998); **62**, R7571(R) (2000); W. Wang, I. Z. Kiss, and J. L. Hudson, Chaos **10**, 248 (2000); M. Wickramasinghe and I. Z. Kiss, PLoS One **8**, e80586 (2013).